Tutor/s

Dra. Eliana Ramírez Rangel
Chemical Engineering & Analytical Chemistry Department

Dr. Javier Tejero Salvador
Chemical Engineering & Analytical Chemistry Department

Grau en Enginyeria Química

Treball Final de Grau

Biomass conversion to bioplastics: determination of thermodynamic properties and equilibrium of the catalysed sorbitol-to-isosorbide double dehydration reaction.

Javier Cuesta Bruned

June 2023

UNIVERSITAT DE BARCELONA

Saber vivir el día a día nos convierte en sabios.

Nach

Primeramente, me gustaría agradecer a mis tutores de este trabajo, la Dra. Eliana Ramírez y el Dr. Javier Tejero por la oportunidad de realizar el trabajo en su grupo de recerca, la ayuda y conocimientos que me han transmitido y más importante el trato personal para conmigo.

Me gustaría agradecer también al resto de docentes del grupo de recerca que me han tendido su ayuda en todo momento.

Agradecer a mis compañeros de laboratorio las horas, risas y comidas compartidas, así como al resto de personas que he conocido en el grado y que hoy puedo llamar amigos.

Por último, quiero agradecer a mi familia, a la que está y a la que estuvo, por el esfuerzo titánico durante años para darme la mejor educación escolar y personal que ha estado en su mano y que me han convertido en la persona que soy.

CONTENTS

SUMMARY

This work, which is part of a larger study, is related to the production of polymers and plastics from biomass (known as biopolymers and bioplastics) as an alternative to the use of fossil fuels derived from petroleum as raw materials on an industrial scale. Specifically, it focuses on the synthesis of isosorbide (IB) from sorbitol (SOH).

Isosorbide is a molecule that has countless applications and uses. It is a monomer for various bioplastics such as poly-(isosorbide carbonate) (PIC), and it participates in the synthesis of pharmaceutical industry or cosmetic formulation intermediates or products. It can also function as an additive for biofuels or various surfactants.

The proposed reaction mechanism to produce isosorbide from sorbitol is the twofold dehydration of sorbitol through 1,4-sorbitan (1,4-ST), catalysed by an acid catalyst. This catalysis is provided by acid solid catalysts, for example ion exchange resins.

This study is dedicated to the experimental determination of the equilibrium constant of the aforementioned reactions over the temperature range 130 - 190 °C, as well as the determination of the thermodynamic properties of the system within this temperature range, including enthalpy, entropy, and Gibbs free energy. These thermodynamic properties will be compared with the existing literature as well as with those obtained through estimation from studies conducted in the same research group.

The enthalpy and entropy changes of the sorbitol dehydration reactions were estimated to be -(7 ± 2) kJ/mol and (15 ± 4) J/(mol·K) and (23 ± 4) kJ/mol and (73 ± 9) J/(mol·K) for 1,4-ST and 2,5-ST formation respectively. As for the IB formation, enthalpy and entropy changes were set to be (15 ± 5) kJ/mol and (46 ± 11). Being the SOH-to-1,4-ST dehydration exothermic and the SOH-to-2,5-ST and 1,4-ST-to-IB reactions endothermic.

Keywords: Isosorbide, sorbitol, thermodynamic properties, equilibrium constant, ion exchange resins, biomass, biopolymers, bioplastics, dehydration.

RESUMEN

Este trabajo, que forma parte de un estudio de mayores dimensiones, está relacionado con la obtención de polímeros y plásticos partiendo de biomasa (conocidos como biopolímeros y bioplásticos) como alternativa a la utilización de combustibles fósiles derivados del petróleo como materia prima a nivel industrial. Más concretamente trata sobre la síntesis de isosorbida (IB) partiendo de sorbitol (SOH).

La isosorbida es una molécula que tiene infinidad de aplicaciones y utilidades, es monómero de diversos bioplásticos como el poli-(isosorbida carbonato) (PIC), está presente en la síntesis de intermedios o productos en la industria farmacéutica y en formulación cosmética. También puede actuar como aditivo de biocombustibles o tensioactivos diversos.

El mecanismo de reacción propuesto para la producción de isosorbida a partir de sorbitol es la doble deshidratación del sorbitol, a través del 1,4-sorbitan (1,4-ST), mediante catálisis ácida. Dicha catálisis viene dada por catalizadores ácidos sólidos, por ejemplo, resinas de intercambio iónico.

Este estudio está dedicado a la determinación experimental de la constante de equilibrio de las reacciones previamente mencionadas en un rango de temperaturas de 130 - 190 °C además de la determinación de las propiedades termodinámicas del sistema en dicho rango de temperatura como son la entalpía, entropía y energía libre de Gibbs. Dichas propiedades termodinámicas se compararán con la literatura, así como con las obtenidas mediante estimación por estudios llevados a cabo en el mismo grupo de recerca.

Las variaciones de entalpía y entropía de las reacciones de deshidratación del sorbitol se estimaron en -(7 ± 2) kJ/mol y (15 ± 4) J/(mol·K), y (23 ± 4) kJ/mol y (73 ± 9) J/(mol·K) para la formación de 1,4-ST y 2,5-ST respectivamente. En cuanto a la formación de IB, se observó que la variación de entalpía y entropía es de (15 ± 5) kJ/mol y (46 ± 11). Siendo la deshidratación de SOH a 1,4-ST exotérmica y las reacciones SOH a 2,5-ST y 1,4-ST a IB endotérmicas.

Palabras clave: Isosorbida, sorbitol, propiedades termodinámicas, constante de equilibrio, resinas de intercambio iónico, biomasa, biopolímeros, bioplásticos, deshidratación.

SUSTAINABLE DEVELOPMENT GOALS

This final project can directly impact the Products and Price offered to customers, as it reduces the use of fossil fuels in production in favour of the use of bio compounds, which reduce emissions and production costs while maintaining product quality. Additionally, some of the different Sustainable Development Goals (SDGs) of the United Nations are met, due to the research on an alternative to fossil fuels and petroleum derivatives, such as the use of biomass for the production of bioplastics. These goals can include SDG 12 and 13.

- SDG 12. Responsible consumption and production: Ensure sustainable consumption and production patterns.
- SDG 13. Climate action: Take urgent action to combat climate change and its impacts.

1. INTRODUCTION

1.1. BIOMASS AS AN ALTERNATIVE TO OIL IN PLASTIC MANUFACTURE

Plastic products have become a ubiquitous part of modern life. Since their wide-scale production in the 1950s, plastics have permeated society due to their use in various applications. Plastic-made materials are central, these can be found widely in everyday products used for clothing, transport, electronic devices, packaging, and more due to their universality and versatility. Plastics have countless social benefits in our daily lives. Population growth, economic progress, commodities, and lifestyle changes are remarkably increasing the demand and production of plastic products.

Plastics, despite being useful products, have a vast number of issues environmentally wise like wildlife pollution, both landmass and oceans, air pollution derived from the usage of fossil fuels, most likely oil, and the emission of toxic and human health threatening compounds like volatile organic compounds [1].

Approximately 90% of plastics produced are derived from fossil feedstocks [2]. Fossil fuels used for plastic production and to power the plastics recycling and resource recovery facilities have significant environmental implications, including greenhouse gas emissions and the depletion of non-renewable resources. Currently, plastic production accounts for approximately 4-8% of oil consumption globally, and this is expected to reach up to 20% by 2050 [2]. These concerns about fossil fuels give rise to seeking an alternative source of energy and materials that might help reduce the carbon footprint, reaching the concept of bioplastics [3].

As it was stated before, conventional plastics are manufactured from fuels like natural gas and petroleum, whereas bioplastics are manufactured by materials derived from natural resources like microbial or plant biomass [3]; such plastics include polylactic acid (PLA),

polyhydroxyalkanoates (PHA), cellulose, starch, and other sugars [2]. Bioplastics are made from renewable polymers, obtained from a biological source, for example, isosorbide, which is obtained from sorbitol, with analogous chemical and mechanical properties to conventional oil-based plastics. Bioplastics show positive aspects environmentally and economically wise in polymer manufacturing. Figure 1 compares the CO_2 recycling cycle for both petrol-based and plant-based plastics [3].

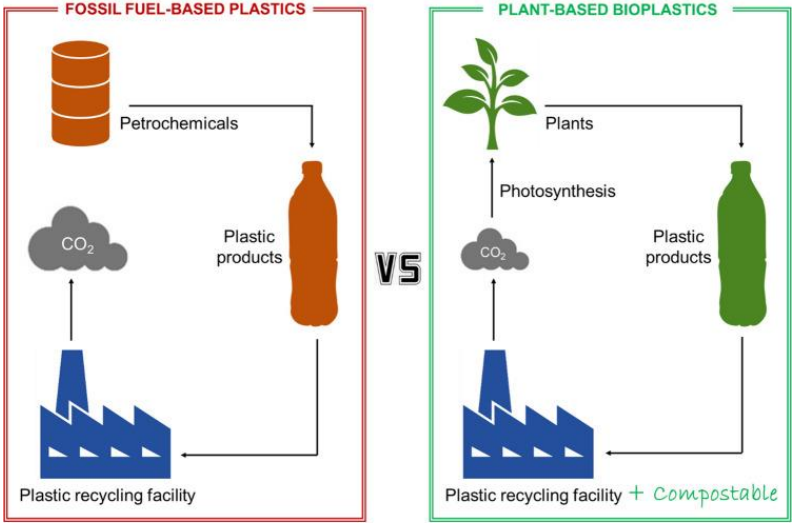

Figure 1. *CO_2 recycling cycle: petrol-based vs plant-based plastics [3].*

Analogously to oil-based plastics, biodegradable biobased plastics can be recycled or incinerated. They may also be microbially degraded, allowing for industrial and home composting, and anaerobic digestion [2].

Biomass mainly consists of lignocellulose, which is a complex biopolymer formed by the combination of lignin, cellulose, and hemicellulose, found in the cell walls of plants. Lignocellulose is the most abundant renewable biomass on earth, which is what makes it one of the most attractive sources for biofuel and bioplastic production. Lignocellulose chemical and biochemical transformation allow the obtention of cellulose derivatives (cellulose acetates, ethers, or esters), glucose and other sugars like sorbitol, biofuels by fermentation like ethanol or butanol, acids like lactic or levulinic, high-value chemicals like phenols, etc.

1.2. SORBITOL-TO-ISOSORBIDE DEHYDRATION REACTION

In recent years, the production of biobased polymers through isosorbide has been gaining increasing attention. Isosorbide ($C_6H_{10}O_4$), which belongs to the isohexide family, is derived from sorbitol, which is a huge renewable feedstock.

Isohexides are chiral V-shaped diols that consist of two fused tetrahydrofuran units with secondary hydroxyl groups. These hydroxyl groups can be in an *endo/endo* configuration (isomannide), *exo/endo* configuration (isosorbide), and *exo/exo* configuration (isoidide) [1]. Figure 2 compares the structures and epimerization of the isohexide family [1].

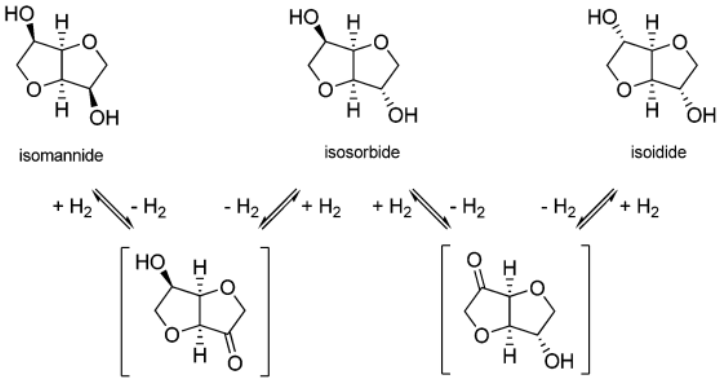

Figure 2. *Isohexides chemical structure and epimerization [1].*

Due to the large availability of bio-based precursors such as sorbitol, glucose, or cellulose, isosorbide is by far the most important of isohexides. Figure 3 shows the isosorbide chemical structure [1].

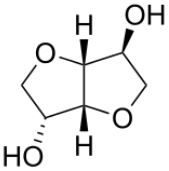

Figure 3. *Isosorbide chemical structure [1].*

As previously mentioned, isosorbide (1,4:3,6-dianhydro-D-glucitol) is an isohexide obtained from sorbitol. The conventional route to isosorbide synthesis involves a sequence of metal-catalysed

hydrogenation of glucose to sorbitol, followed by the twofold acid-catalysed dehydration of sorbitol through 1,4-sorbitan.

Isosorbide is a monomer for several bioplastics, including poly-(ethylene-co-isosorbide) terephthalate (PEIT), poly-(isosorbide carbonate) (PIC), and poly-(isosorbide oxalate), also is commonly used in the synthesis of pharmaceutical intermediates like isosorbide dinitrate, for cosmetic formulation like dimethylisosorbide, or synthesis of fuel additives and surfactants [1-4].

Sorbitol ($C_6H_{14}O_6$), also known as D-sorbitol or D-glucitol is a polyalcohol constituted by six atoms of carbon and six hydroxyl groups as it is shown in Figure 4. This sugar alcohol, which has the biggest market share among the sugar alcohols, is present in the food and pharmaceutical industry due to its sweetness (60% of sucrose sweetness), its low-caloric properties, laxative and humectant properties, as well as chemical preparations apart of isosorbide like vitamin C [1]. Figure 4 shows sorbitol's chemical structure [5].

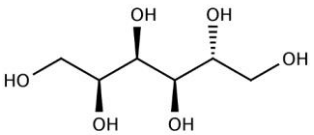

Figure 4. *Sorbitol chemical structure [5].*

As previously stated, sorbitol is synthesized by the hydrogenation of glucose, however, it can be obtained through cellulose in the presence of noble metals and transition metal-based catalysts, as well as by the reduction of glucose and fructose in addition to a certain group of bacteria [5]. Figure 5 shows the reaction mechanism of the hydrogenation of glucose to sorbitol [5].

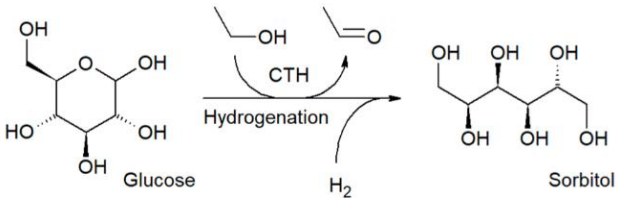

Figure 5. *Glucose to sorbitol hydrogenation reaction mechanism [5].*

The sorbitol-to-isosorbide dehydration is a two-stage acidly catalysed reaction that goes through 1,4-sorbitan. Despite that, 1,4-sorbitan is not the only intermediate molecule formed in the first sorbitol dehydration, 1,5-sorbitan, 3,6-sorbitan, and 2,5-sorbitan can also be formed as presented in Figure 6. Among these anhydrosorbitols shown in Figure 6, some other compounds can be formed like 2,6-sorbitan, 2,5-mannitan, and 2,5-iditan, which are laid out in Figure 7. Despite all those possible reaction paths, only the ones involving 1,4-sorbitan and 3,6-sorbitan lead to isosorbide by the dehydration of the mentioned intermediates [5].

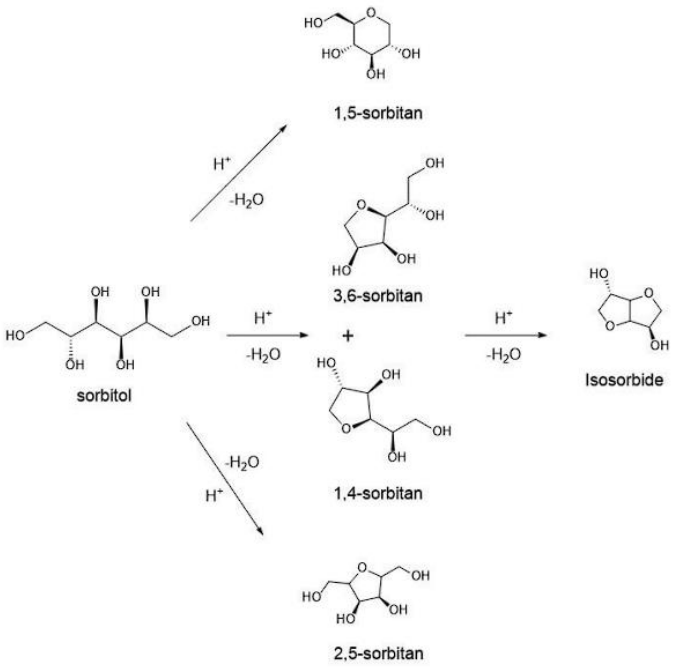

Figure 6. *Sorbitol-to-isosorbide reaction mechanism with subproducts formation [5].*

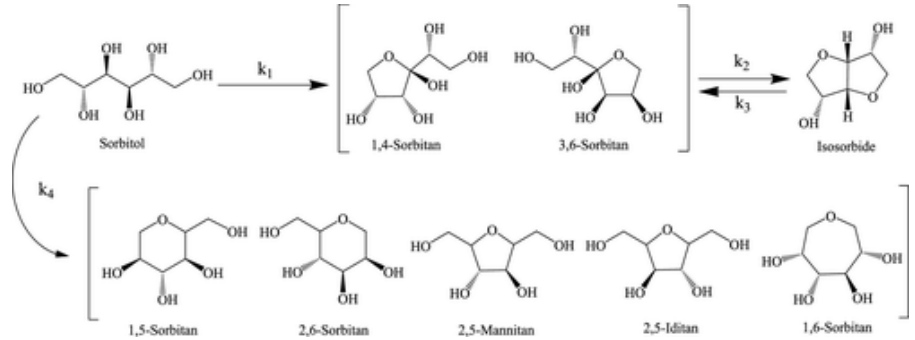

Figure 7. *Sorbitol-to-isosorbide reaction mechanism with subproducts formation [5].*

Of all the possible subproducts formed, the ones whose yield is higher for 1,4-sorbitan and 2,5-sorbitan rather than the rest of the species formed, which are undesired (except for 3,6-sorbitan) because none of them lead to isosorbide. This non-desired anhydro-compounds formation depends on the experimental conditions at which the experimental run is taken place like pH, catalyst type, stirring, or time of reaction.

1.3. ION-EXCHANGE RESINS AS CATALYSTS FOR DOUBLE SORBITOL DEHYDRATION

As aforementioned at 1.2, sorbitol-to-isosorbide double dehydration is acid-catalysed. This type of acid catalyst used for the isosorbide production might affect the yield to isosorbide of the sorbitol dehydration. Despite some homogeneous catalysts, those that exist in the same phase as the reactants, show good catalytic activity in isosorbide production, many problems on an industrial scale appear by their usage such as corrosion, or side product formation. Due to this problems, heterogeneous acid catalysts are preferred industry-wise. Table 1 gathers a summary of some acid ion-exchange resins proposed for sorbitol-to-isosorbide reaction system. This table shows some of the available catalysts for a sorbitol-to-isosorbide reaction, as well as reaction conditions like the solvent used and temperature, and the conversion and selectivity of the process.

Table 1. *Summary of some catalytic systems proposed for sorbitol-to-isosorbide reaction [1].*

Catalyst	Reaction conditions		Selectivity [%]	Conversion[d] [%]	Ref.
	Solvent[a] (M)	T [°C]			
Amberlyst-36	H_2O (13,5)	150	69	100	[25]
Hβ-75	H_2O (0,5)	200	77	100	[26]
Hβ-75	Free	127	76	100	[27]
Glu-Fe_3O_4-SO_3H	Free	140	94	100	[28]
SAC-13[b]	Free	130	83	100	[29]
Dowex-50WX2	Free	130	78	100	[29]
Amberlyst-15	Free	130	67	100	[29]
Deloxan	Free	130	68	100	[29]
SHTC	Free	130	80	100	[29]
SiO_2-SO_3H	Free	120	84	100	[30]
SBA15-$PrSO_3H$	Free	150	78	90	[31]
SBA15-$ArSO_3H$	Free	170	71	100	[32]
B phosphate	H_2O[c]	250	80	99	[33]
Zr phosphate	Free	210	73	100	[34]
MST-450	Free	180	70	100	[35]
BIL-5	Free	130	85	99	[36]
$Bi(OTs)_3$	Free	145	67	100	[37]
Hβ-20	MIBK (0,4)	170	93	100	[38]

[a] Reaction solvent, substrate concentration (M) in brackets. [b] Nafion-silica composite. [c] Sorbitol 70 wt%. [d] Substrate conversion.

Those acid catalysts, which work like Bronsted acids, cannot be dissolved in the reaction medium. Despite the many acid catalysts that can be used in biopolymer production like zeolites, silica-alumina, and transition metal oxides, this experimental workout will only focus on ion-exchange resins as an acid catalyst.

Ion-exchange resins or IER are solid organic materials, that exchange ions of their structure with those of another polar solution with which they come into contact, whose composition is a polymeric matrix of carbon-hydrogen chains with functional groups. The tridimensional C-H structure is hydrophobic, and the functional groups attached to that chin are normally hydrophilic. This structure makes the resins insoluble in solvents that do not break the bonds between two carbon atoms like water [6].

Many aromatic vinyl compounds such as polystyrene-divinylbenzene (PS-DVB), vinyl toluene, vinyl chlorobenzene, or vinyl naphthalene among others are common types of IER. These resins are obtained by the copolymerization of styrene and divinylbenzene. Despite existing acid, basic, redox, and metallic catalysts, acid catalysts will be the focus of the study, being those induced a strong acidic behaviour by a sulphonation process with sulphuric acid. Figure 8 shows the chemical structure of a polystyrene-divinylbenzene matrix after sulfonation [6].

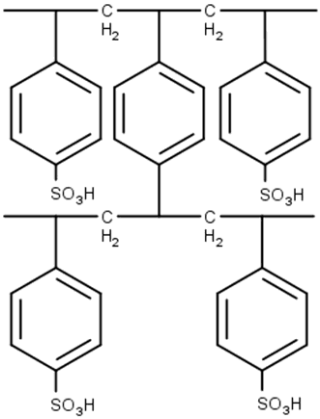

Figure 8. *Chemical structure of a polystyrene-divinylbenzene matrix after sulfonation [6].*

Resin properties depend on the monomer, the method of polymerization, and the functional groups attached to the resin matrix nature. Some of those properties are:

- Functionalization degree. Representing the percentage of aromatic rings functionalized.
- Ion-exchange capacity. The number of fractional groups that the resin can introduce in catalysed reactions.
- Surface area. Particle total surface, including internal and external pores, per gram of dry solid.

- Porosity. percentage of void spaces, or pores, in a material
- Swelling degree. Solvent absorption by the resin, the resin goes from a dry state to a swollen state. Swelling is way pronounced in polar solvents like alcohols or water. Several factors involve the swelling phenomenon such as temperature, the crosslinking degree, the solvent characteristics, etc.
- Moisture content. The ratio of water weight within the resin and the total hydrated resin weight.
- Pore volume. Volume of pores per gram of dry solid, those pore, depending on the pore diameter (d_{pore}), can be micro (< 2 nm), meso (2 nm > d_{pore} > 50 nm) or macropore (< 50 nm).

In previous work done at the same research group, specifically: "A contribution to the study of the fructose to isosorbide conversion reaction" made by Laura Castro Santacreu [7], has been observed that acidic ion-exchange resins like Amberlyst-45 (A-45) and Purolite CT-482 (CT-482). This resins had a commercial pore diameter and performed the reactions at a range of temperatures oscillating between 120 and 170 °C for A-45 and 120 and 190 °C for (CT-482) respectively and at 30 bar operation pressure. One gram of catalyst was used in experimental runs of 8,5 hours for a starting reactant composition without isosorbide and in a highly diluted in deionized water system in which the equilibrium was not always reached. Despite not always reaching the equilibrium, these conditions are adopted in the present experimental study, forcing the system to reach the equilibrium making the experimental runs last a considerable number of hours, using a higher amount of catalyst and performing some of this runs with product in the starting mixture. It is also worth of mention that conversions between 87 and 97% are observed as well as a selectivity to isosorbide oscillating between a 24 and 57%.

2. OBJECTIVES

This experimental work belongs to a study about the obtention of polymer molecules from biomass.

This study's main objective is to experimentally estimate the thermodynamical properties of the sorbitol-to-isosorbide dehydration system, catalysed with acid ion-exchange resins, and compare those properties with previous experimental data, computational studies, and theoretical estimations.

3. THEORETICAL FRAMEWORK

3.1. EQUILIBRIUM CONSTANT DETERMINATION

The chemical equilibrium is the condition, in the course of a chemical reaction, in which the amount, quantified as concentration, molar fraction, or partial pressure (gas phase), of reactants and products, suffer no net change. At equilibrium, the reaction rate tends to zero and the reaction can be considered as completed.

The equilibrium constant in an ideal system can be calculated by the usage of the mass-action ratio (Γ_x), which is the ratio between the molar fractions of the involved reactants at the studied reaction. In a non-ideal system, the mass-action ratio must be related to the activity (a_i) of each compound. For this activity ratio, besides the molar fraction ratio, the activity coefficient (γ_i) must be considered, as shown in Equation 1.

$$\Gamma_a = \Gamma_\gamma \cdot \Gamma_x = \prod_{j=1} (a_j)^{\upsilon_j} = \prod_{j=1} (\gamma_j)^{\upsilon_j} \cdot \prod_{j=1} (x_j)^{\upsilon_j} \quad (1)$$

where Γ_a and Γ_γ are the mass-action ratio of the activities and the activity coefficients respectively and υ_j is the stoichiometric coefficient of each one of the "j" species.

The activity coefficients are the ratio of a component's fugacity in a mixture to the fugacity of an ideal solution of the same composition [8]. These are calculated following the modified UNIFAC-Dortmund method explained later on. Fugacity is a measure of chemical potential.

The fugacity of a chemical in a given phase is defined as the vapor pressure the chemical would have in a gas volume at equilibrium with the phase [9].

When the equilibrium is reached, as the composition remains constant with time, the mass-action ratio equals to the chemical equilibrium constant, so $\Gamma_x = K_x$, $\Gamma_\gamma = K_\gamma$ and $\Gamma_a = K$, K is the thermodynamic equilibrium constant and is obtained by:

$$K = K_\gamma \cdot K_x \tag{2}$$

3.2. MOLE FRACTION EQUILIBRIUM CONSTANT DETERMINATION

For a known reversible reaction like:

$$aA + bB \rightleftharpoons cC + dD$$

where A, B, C, and D are the reactant species and the products involved in the reaction and a, b, c, and d are their respective stoichiometric coefficient.

The equilibrium constant, at an ideal system, can be obtained like:

$$\Gamma_x = K_x = \prod_{j=1} (x_j)^{\upsilon_j} \tag{3}$$

The equilibrium can otherwise be stated as the ratio of concentrations K_c (Equation 4) and the ratio of partial pressure (gas state reaction) K_p (Equation 5):

$$K_c = \prod_{j=1} (c_j)^{\upsilon_j} \tag{4}$$

$$K_p = \prod_{j=1} (p_j)^{\upsilon_j} \tag{5}$$

3.3. ACTIVITY COEFFICIENT CONSTANT DETERMINATION

3.3.1. Modified UNIFAC-Dortmund activity coefficient determination

For the description of multicomponent non-electrolyte systems, g^E-models or equations of state binary data can be applied alone. Experimental data are however often missing. In such cases group contribution methods such as ASOG (Derr and Deal, 1969; Kojima and Tochigi, 1979) or UNIFAC (Fredenslund et al., 1975, 1977) can be successfully applied. These methods are developed for the prediction of group interaction parameters in the equilibrium phase for both vapor-liquid equilibrium (VLE) and liquid-liquid equilibrium (LLE).

In the modified UNIFAC-Dortmund model, as in the original UNIFAC model, the activity coefficient (γ_i) is the sum of a combinatorial part (γ_i^C), which takes account of the form and size of the molecules and its occupied volume in the reaction medium, and a residual part (γ_i^R) which sums up the activity coefficient temperature dependence and the intramolecular group interaction of each molecule studied, stated as:

$$\ln(\gamma_i) = \ln(\gamma_i^C) + \ln(\gamma_i^R) \tag{6}$$

In the modified UNIFAC model the combinatorial contribution to the overall activity coefficient is obtained, in an empirical way to deal with very different size compounds, by the application of the Equation 7.

$$\ln(\gamma_i^C) = 1 - \Phi_i' + \ln(\Phi_i') - 5q_i\left(1 - \frac{\Phi_i}{\theta_i} + \ln\left(\frac{\Phi_i}{\theta_i}\right)\right) \tag{7}$$

where the parameters Φ'_i, Φ_i and Θ_i can be calculated, by the relative group van der Waals volumes (R_k) and surface areas (Q_k), like:

$$\Phi_i' = \frac{r_i^{3/4}}{\sum_j x_j r_j^{3/4}} \tag{8}$$

$$\Phi_i = \frac{r_i}{\sum_j x_j r_j} \tag{9}$$

$$\theta_i = \frac{q_i}{\sum_j x_j q_j} \tag{10}$$

where:

$$r_i = \sum_k \upsilon_{k,i} R_k \tag{11}$$

$$q_i = \sum_k \upsilon_{k,i} Q_k \tag{12}$$

where the subscript "i" refers to the molecule studied, "j" refers to all the molecules in study including the one that is referred to as "i" and the subscript "k" refers to each group that is present in the molecule of study. The $\upsilon_{k,i}$ refers to the number of "k" groups in the species "i". Rk and Qk values are tabulated at different UNIFAC and modified UNIFAC papers found in the bibliography of this work [12-13-14-15].

The residual contribution can be obtained by:

$$\ln(\gamma_i^R) = \sum_k \upsilon_{k,i} \left(\ln(\Gamma_k) - \ln(\Gamma_k^*)\right) \tag{13}$$

where Γ_k is the group residual activity coefficient, and Γ_k^* is the residual activity coefficient of group "k" in a reference solution containing only molecules of type "i". These residual activity coefficients can be found following Equations 14 and 15.

$$\ln(\Gamma_k) = Q_k \left(1 - \ln\left(\sum_m \Theta_m \Psi_{mk}\right) - \sum_m \frac{\Theta_m \Psi_{km}}{\sum_n \Theta_n \Psi_{nm}}\right) \tag{14}$$

$$\ln(\Gamma_k^*) = Q_k \left(1 - \ln\left(\sum_m \Theta_m^* \Psi_{mk}\right) - \sum_m \frac{\Theta_m^* \Psi_{km}}{\sum_n \Theta_n^* \Psi_{nm}}\right) \tag{15}$$

On one hand the subscript "k" refers to the studied group and subscripts "n" and "m" refer to the rest of the groups found in the studied molecule. On the other hand, Θ_m and Θ_m^* are the group area fraction and the group are fraction for the aforementioned reference state respectively and are given by the following:

$$\Theta_m = \frac{Q_m X_m}{\sum_n Q_n X_n} \tag{16}$$

$$\Theta_m^* = \frac{Q_m X_m^*}{\sum_n Q_n X_n^*} \tag{17}$$

being X_m the group mole fraction and X_m^* the group mole fraction for the reference state and are calculated by:

$$X_m = \frac{\sum_i \upsilon_{m,i} x_i}{\sum_j \sum_n \upsilon_{n,j} x_j} \tag{18}$$

$$X_m^* = \frac{\upsilon_{m,i}}{\sum_j \upsilon_{m,j}} \tag{19}$$

where x_i is the molar fraction of the compound in study and x_j the molar fraction each of the molecules in study, including molecule "i".

In the UNIFAC-Dortmund modified method the temperature-dependent interaction parameters introduced into the residual part, Ψ_{nm}, are obtained following:

$$\Psi_{nm} = \exp\left(-\frac{a_{nm} + b_{nm}T + c_{nm}T^2}{T}\right) \tag{20}$$

where a_{nm}, b_{nm} and c_{nm} interaction parameters between groups are found the same way as R_k and Q_k, previously mentioned.

3.3.2. Activity coefficient equilibrium constant determination

At a non-ideal system, once γ_i is known and for the same known reversible reaction defined at 3.2,

$$aA + bB \rightleftharpoons cC + dD$$

the equilibrium constant, can be obtained like:

$$\Gamma_\gamma = K_\gamma = \prod_{j=1} \left(\gamma_j\right)^{\upsilon_j} \tag{21}$$

3.4. PRESSURE EFFECT ON THE EQUILIBRIUM CONSTANT: POYNTING CORRECTION FACTOR

Previous equations were deduced considering that the fugacity of the liquids in study depends in a weak manner on pressure, however, when working at high pressures this assumption can be inaccurate.

To check if the high pressure produces a deviation in the equilibrium constant the Poynting correction factor must be evaluated following the expression quoted in “Smith and Van Ness”, 1987 [16]:

$$K_{\Gamma_i} = \exp\left(\frac{P-1}{RT}\right) \cdot \sum_{j=1} \upsilon_{ij} V_j \tag{22}$$

where P is the working pressure in atm because the pressure reference is stated as 1, and V_j is the liquid molar volume in L/mol of the “j” compound. T is the temperature in Kelvin degrees and R is the ideal gas constant 0,08206 in (atm·L)/(K·mol) and υ_j is the stoichiometric coefficient of each one of the “j” species.

The liquid molar volume (V_j) is determined by the usage of Le Bas additive method, which obtains de liquid molar volume by addition of the molar volume of each atom present in the studied molecules [17].

If the pressure affects the thermodynamical equilibrium K values must be corrected like:

$$K = K_\gamma \cdot K_x \cdot K_\Gamma \tag{23}$$

3.5. THERMODYNAMICAL PROPERTIES DETERMINATION

The thermodynamics of a reaction or thermochemistry, which studies the heat exchange and the work governed by the laws of mass, momentum, and energy conservation, is defined through properties like the enthalpy, entropy, and Gibbs free energy.

Firstly, enthalpy, H, is the sum of the internal energy and pressure times volume of a thermodynamic system. Enthalpy cannot be measured but enthalpy changes (ΔH) can, this enthalpy change is equal to the change of internal energy (ΔE) plus pressure-volume work (PΔV). Enthalpy exhibits characteristics akin to energy and is considered a property or state function. It possesses energy units (joules or ergs) and its precise value is solely determined by the system's temperature, pressure, and composition, without any influence from its past history [18].

Secondly, entropy, S, is the measure of a system’s thermal energy per unit temperature that is unavailable for doing useful work. Because work is obtained from ordered molecular motion,

entropy serves as a quantification of the level of molecular disorder, disarray or randomness present within a given physical or biological system. When the entropy of a system increases, it signifies a decrease in the amount of information available to describe or predict the state of the system [19-20].

Lastly, free energy is a property or state function of a system that has reached its thermodynamic equilibrium and has energy dimensions. Free energy is characteristic of a system and is influenced by the amount of substance present in a given thermodynamic state. It is considered to be an extensive property, meaning its value depends on the quantity of the substance. By analysing changes in free energy, is possible to determine spontaneous changes direction and evaluate the maximum work that can be obtained from various thermodynamic processes, including chemical reactions [21].

Once a reaction reaches the equilibrium and the equilibrium constants, at different temperatures, are calculated, both the enthalpy and the entropy of the reaction can be obtained by van't Hoff,

$$\frac{dlnK_i}{dT} = \frac{\Delta_r H_i^\circ}{RT^2} \tag{24}$$

As Gibbs free energy can be calculated like:

$$\Delta_r G_i^\circ = \Delta_r H_i^\circ - T \cdot \Delta_r S_i^\circ \tag{25}$$

Then, van't Hoff equation (Equation 24) can be restated and linearized like:

$$\ln(K_i) = -\frac{\Delta_r G_i^\circ}{RT} = -\frac{\Delta_r H_i^\circ}{R} \cdot \left[\frac{1}{T}\right] + \frac{\Delta_r S_i^\circ}{R} \tag{26}$$

where $\Delta_r G_i^\circ$, $\Delta_r H_i^\circ$ and $\Delta_r S_i^\circ$ are the standard Gibbs free energy, enthalpy and entropy increment for each reaction "i", K is the equilibrium constant as previously mentioned.

4. EXPERIMENTAL SECTION

4.1. MATERIALS

To conduct the sorbitol-to-isosorbide dehydration reaction both ≥99,5% purity sorbitol (Sigma-Aldrich - Life Science Products, CAS: 50-70-4) jointly with 98% purity isosorbide (Alfa Aesar, CAS: 652-67-5) have been used, as well as deionized water (Mili-Q, Millipore).

In addition, ≥99% purity 1,4-sorbitan (Sigma-Aldrich - Life Science Products, CAS: 27299-12-3) has been used for identification and quantification of the species.

Besides the used reactants and calibration compounds, 99,9995% Stickstoff Nitrogen supplied by Linde has been used to pressurize the stirred batch reactor. The dehydration reaction is catalysed by Purolite CT-482 (Batch: 3804Q/13/6) or Amberlyst-45 (Batch: 45-2201002) ion-exchange resin.

Table 2 presents some of the main physical properties of the ion-exchange catalysts utilized in the present study [6]:

Table 2. *Main physical properties of the tested ion-exchange resins as catalysts.*

Catalyst	**Type**	**DVB** [%][a]	**Acid capacity** [$eqH^{+}\cdot kg^{-1}$]	**Bead diameter,** d_b [mm]	**Moisture** [%]	**Max. Operating Temperature** [°C]
A-45	macro	medium	3,65	0,58-0,75	49-54	170
CT-482	macro	low	3,65	0,81	48-58	190

[a] *Crosslinking degree classification: low (7-12%); medium (12-17%).*

4.2. EQUIPMENT

The experimental equipment is divided into two devices: the reaction equipment and the analytical system.

4.2.1. Reaction equipment

The equipment required to carry out the dehydration reaction consists of a torispherical bottomed stainless steel (316 SS) 100 mL stirred batch reactor, (provided by Autoclave Engineers), supported by a 316 SS cylindrical ring-shaped backup and a rubber gasket to seal the top of the reactor, which operates at a manometer pressure of 30 bar. Figures 9 and 10 show the reaction equipment.

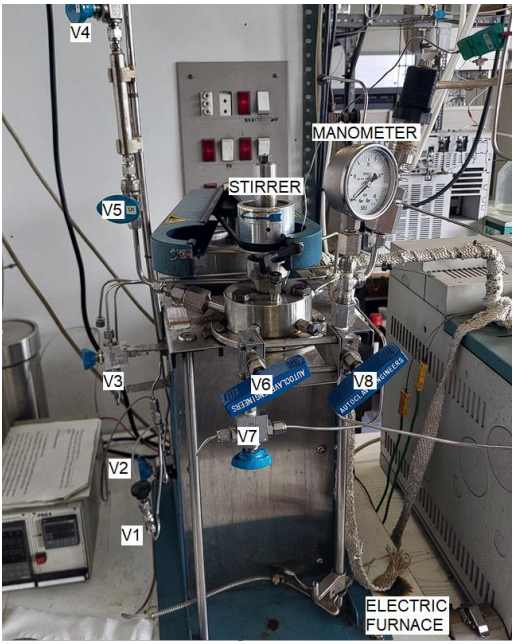

Figure 9. *Reaction equipment: valves, manometer, stirrer, and electric furnace heater.*

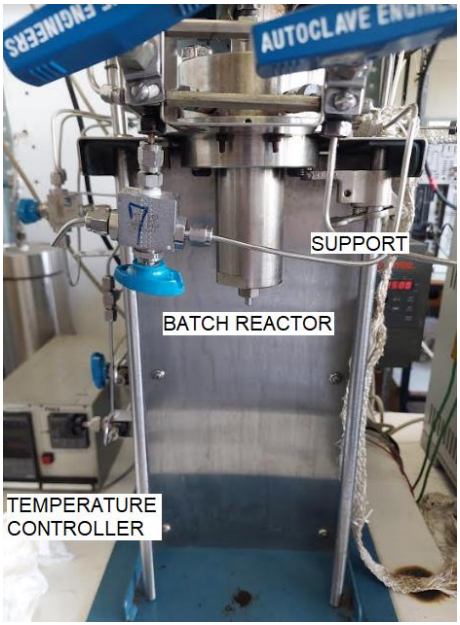

Figure 10. *Reaction equipment: batch reactor and temperature controller.*

This manometer (EN837-1) is placed between the reactor and the reactor's relief valve (V8).

As shown in Figures 9 and 10, valves V3, and V6, both the three-way valves provided by Autoclave Engineers, and V7 also a three-way valve, provided by Hoke, are manually operated to extract samples. Between valve V6 and the reactor, there is a filter that avoids losing catalyst particles by sampling. Nitrogen to pressurize the tank is provided through valves V1 (needle valve provided by Whitey) and V3.

The reactor heating system consists of an electric furnace, which makes the reactor function as a jacketed reactor, connected to a PID temperature control system (TC 22 temperature) by two temperature sensors, one measures the reactor's internal temperature while the other one measures the reactor's wall temperature. This temperature controller reaches a setpoint and maintains the temperature inside the batch reactor constant, with an error of ± 0,1 °C.

Finally, the stirred batch reactor contains an agitation system composed of four stirring blades that connect to a mechanical rotor (MagneDrive II Series 0,7501). This mechanical rotor is connected to a stirring speed controller (T-VERTER N2-SERIES 220V-0,4 kW). To improve the mixture homogenization there is a baffle placed close to the stirring paddles.

4.2.2. Analytical system

Samples are taken from the reactor and injected for analysis at a high-performance liquid chromatograph or HPLC (Agilent Technologies 1200 Infinity Series, 1260 Infinity), with an Agilent Hi-Plex Ca-packed column with a 4,6 mm diameter and 250 mm length. This column works at 80 °C, 36 bar, and uses deionized Millipore water as a mobile phase.

Both the mobile phase and the sample are pumped into the column by a quaternary pump at a 0,3 mL/min flow rate.

Once the sample exits the column, enters a refractive index detector or RID also provided by Agilent, that works at a temperature of 35 °C, which detects the species that differ from the mobile phase and shows an area related to the concentration (g/mL) through the calibration equations, previously obtained by the research group, displayed at Table 3.

Table 3. *Calibration of the species present in the sorbitol-to-isosorbide double dehydration system.*

Species	Retention time [min]	Calibration equation[a]	Calibration R^2
Sorbitol	7,822	y = (1,48E-09 ± 7,1E-12)x + (6,88E-05 ± 6,6E-05)	0,999
Isosorbide	8,666	y = (2,00E-09 ± 2,0E-11)x + (2,00E-05 ± 1,0E-4)	0,997
1,4-Sorbitan	10,258	y = (1,91E-09 ± 1,0E-10)x + (1,42E-03 ± 6,7E-04)	0,995
2,5-Sorbitan	13,359	y = (1,91E-09 ± 1,0E-10)x + (1,42E-03 ± 6,7E-04)	0,995

[a] *In the calibration equations "y" refers to the concentration of the species in g/mL and "x" refers to the measured area [-] by the RID.*

4.3. PROCEDURE

4.3.1. Reactor loading and assembly

Initially, the reactant and the main aimed product, sorbitol, and isosorbide respectively, are weighed at a Pioneer PX analytical balance, provided by Ohaus, with a precision of ± 0,0001 g.

Deionized water is also weighed as the solvent of the solution and added to an Erlenmeyer flask with the reactants previously weighed.

Once the reaction solution is prepared the catalyst is taken out of the oven. The ion exchange resin was placed in the oven at 110 °C and a minimum of twenty-four hours before the reaction solution preparation. The catalyst is weighed the same way as the reactants, and it is added to the reactor vessel. When the catalyst is in the batch reactor, the reaction solution is added to it and the assembly procedure begins, placing the reactor vessel in the reactor support and screwing three safety screws. The process must be fast since the resin is extremely hygroscopic, and the system should not add moisture from the environment because the amount of water added to the reaction system is already measured.

Formerly, with the reactor assembled, a tightness test takes place, filling with soap foam or anti-leakage foam every rabbet and slot and pressurizing the reactor carefully. In order to pressurize the reactor, once valve V8 is completely closed, valve V1 is opened and valve V3 is set in position one, which allows the entrance of the inert gas into the system, valve V3 is then closed.

After the tightness test is done, and the vessel is pressurized, the reactor is jacketed with the electric furnace, once it is fastened the temperature control system is connected. Both reactor and vessel wall temperatures are set as a setpoint, and the heating starts. Once everything is tightened and started, the stirring is connected.

4.3.2. Sampling and analysis

Samples are taken at 1,5 mL sample vials. The sampling procedure starts by placing valve V7 in position 1. Afterward, valve V6 is slowly opened until a quarter of the vial is filled with the reactor's inner solution. Once the sample is taken V6 is closed and V7 is placed at position 2.

After taking a sample there is a need to recover the sample stuck in the pipe between V6 and the reactor vessel. Valve V3 is placed in position three, towards the sample-taking valves, and relief valve V8 is opened until the pressure inside the batch reactor is 10 bar. Once this pressure is reached V8 is closed fast, and equally rapid V6 is opened until the pressure rises to 30 bar and then closed. This procedure is repeated at least three times. Right after V7 is

repeatedly opened and closed to clean both the valve and the pipe between V7 and the open air.

This complete procedure is followed for every sample taken. Besides de sample taken before the addition of the reaction mixture to the reaction system, the first sample is taken when the thermal equilibrium (setpoint temperature) is reached, and the time this sample is taken is set as the start of the reaction time (t=0). Due to the fact that the aim of the experiments is the study of the thermodynamic properties, and the chemical equilibrium must be reached, there is no time set for any of the runs, so one sample is taken an hour after the first one is taken and the next one between 1 or 2 hours later. Next samples are taken one day after, now every hour, if the reaction does not seem to have reached the equilibrium yet, the run will last until the next day, when, like the previous day samples will be taken each hour. The experimental run comes to an end when 3 or more consecutive samples show close results at the HPLC.

Right after a sample is taken it is diluted 1:2 in another sample vial, adding 210 µL of the sample and 210 µL of deionized water. Once the dilution is prepared and the flow rate at the HPLC is set at 0,3 mL/min 50 µL of the diluted sample are injected into the Ca-packed column.

4.3.3. Reactor and HPLC cleaning and disassembly

Once the last sample is analysed, and the experimental run comes to an end, one last sample is taken, and both the heating and the agitation are stopped. While the reactor is being cooled down at room temperature, the HPLC water flow rate is lowed from 0,3 to 0,1 mL/min and is also cooled down to room temperature. To clean and decompress the Ca-packed column it is flipped so the flow inside the column goes the opposite direction. The column is also cleaned with a 20% solution of acetonitrile.

After the reactor is cooled down, the electric furnace is unfastened and taken off the reactor. Valve V8 is opened to relieve the pressure inside the vessel. When the reactor is perfectly depressurized reactor can be disassembled, by unscrewing the three screws and taking the vessel off the reactor support. The remaining reaction solution is filtered with laboratory filter paper and a laboratory funnel. The catalytic solid, once filtered is thrown into the corresponding waste container. The reactor is cleaned with deionized water, filled up with water, and assembled again. Before the new assembly nitrogen is forced to flow through the equipment

pipes to clean up those pipes. Once the reactor is reassembled it is pressurized and heated up to 60 °C and the process of sampling is repeated 5 times to clean the sampling pipes and valves.

Finally, the reactor is cooled down and depressurized again and fully disassembled and dried up.

4.4. EXPERIMENTAL CONDITIONS

Each run was carried out at a different temperature, to study how the chemical constant and then the thermodynamical properties change with the temperature, the range of those oscillating between 130 and 190 °C. At every experimental run the temperature was kept constant. The reaction time of each experiment has been different, however, the average time for each run has been between 2800 and 3300 minutes (47 – 55 hours), this time is set by the results obtained at the HPLC, when the value obtained at the analysis repeats itself a minimum of 3 times, within a small deviation, means that the equilibrium is reached, and the experiment can end. The operation pressure is 30 bar, and remains constant for every run, due to the fact that inside the reactor there is an aqueous solution, and at temperatures above 100 °C it is not possible to work at atmospheric conditions. This conditions are obtained from "A contribution to the study of the fructose to isosorbide conversion reaction" made by Laura Castro Santacreu [7] as aforementioned.

On one hand, the initial sorbitol concentration in each experimental run is kept constant. The added mass of sorbitol is around 1,75 g in each experiment and 70 mL of deionized water, which means that the theoretical concentration of sorbitol is around 0,025 g/mL. On the other hand, the initial isosorbide concentration varies through the experiments, going from 0 to 0,023 g/mL (0 to 1,6 g of isosorbide). The isosorbide initial concentration has been changed to accelerate reaching the equilibrium in some of the experimental runs.

As well as the initial concentration of the reactant (SOH), the stirring speed is maintained constant during all the experimental workout at 500 rpm, and the catalyst mass has been fixed at 5 g for all the experimental runs. This may change at some experiments previously realized at the research group.

Table 4 shows all the experimental runs carried out, and its conditions, so as to study the thermodynamical properties.

Table 4. *Experimental runs.*

RUN	CATALYST	T [°C]	$m_{sorbitol}$ [g]	$m_{isosorbide}$ [g]	m_{H2O} [g]	$m_{catalyst}$ [g]	Stirring [rpm]
E33J	CT-482	130	1,7519	1,0441	70,2536	5,0059	500
E37J	CT-482		1,7506	1,0050	70,0679	5,0056	500
E31J	CT-482	140	1,7506	1,2057	70,1891	5,0106	500
E32J	CT-482		1,7517	1,2118	70,1034	5,0011	500
E28J	CT-482	150	1,7533	---	70,0721	5,0188	500
E29J	CT-482		1,7505	---	70,1321	5,0206	500
E15	A-45		1,7538	---	70,7030	5,0045	500
E16	A-45		1,7521	---	70,0620	5,0580	500
E30J	CT-482	160	1,7522	1,6220	70,2757	5,0063	500
E14	A-45		1,7505	---	70,4080	5,0125	500
E21	A-45		1,7500	---	70,0330	5,1363	500
E26J	CT-482	170	1,7524	---	70,7196	5,0579	500
E27J	CT-482		1,7536	---	73,6623	5,006	500
E12	A-45		1,7511	---	70,2070	5,0191	500
E19	CT-482		1,7556	---	70,2280	5,1776	500
E22	CT-482		1,7532	---	70,7260	5,7063	500
E17	CT-482	180	1,7523	---	70,1370	3,0270[b]	500
E20	CT-482		1,7521	---	70,1260	5,7281	500
E25	CT-482		3,5069[a]	---	70,5490	5,5625	500
E18	CT-482	190	1,7556	---	70,2280	5,1776	500
E23	CT-482		3,5281[a]	---	70,2170	5,2776	500

[a] These experimental runs have a different initial SOH mass. [b] These experimental runs have a different catalyst mass.

5. RESULTS AND DISCUSSION

5.1. MONITORING OF AN EXPERIMENT

The experimental run E26J, taken place at 170 °C and carried out with 5,0579 g of CT-482 catalyst, 1,7524 g of sorbitol, no initial isosorbide, and a volume reaction of 70,7196 mL of water, is used to present the experimental results. The following is repeated for each run.

Once the samples of the experiment, each one belonging to a different reaction time, have been analysed at the HPLC, the concentration in mol/L for each sample has been found after transforming the measured areas in a concentration of g/mL using the calibration equations shown at Table 3, and respectively transformed to a mol/L concentration. Table 5 shows the concentration (mol/L) and the reaction time for each sample measured.

Table 5. *SOH, IB, 1,4-ST, 2,5-ST and H_2O concentration (mol/L) for each reaction time.*

t [min]	C_{SOH} [mol/L]	C_{IB} [mol/L]	$C_{1,4\text{-}ST}$ [mol/L]	$C_{2,5\text{-}ST}$ [mol/L]	C_{H20} [mol/L]
0	0,1078	0,0177	0,0173	0,0173	55,5556
0	0,1112	0,0066	0,0349	0,0194	55,5642
59	0,0186	0,0669	0,0919	0,0270	55,6891
127	0,0042	0,0697	0,0876	0,0276	55,6882
1640	0,0028	0,1487	0,0514	0,0305	55,7339
1700	0,0032	0,1804	0,0539	0,0336	55,7711
1760	0,0031	0,1984	0,0577	0,0355	55,7949
2890	0,0031	0,2207	0,0665	0,0396	55,8301
2953	0,0031	0,2397	0,0659	0,0399	55,8489
3010	0,0031	0,2261	0,0608	0,0377	55,8280
3080	0,0030	0,2274	0,0628	0,0388	55,8324

After these concentrations are obtained, and conducting all the necessary transformations, the mole fraction of each reactant is obtained and represented against the reaction time at a figure like Figure 11 in order to discuss whether the chemical equilibrium is reached or not.

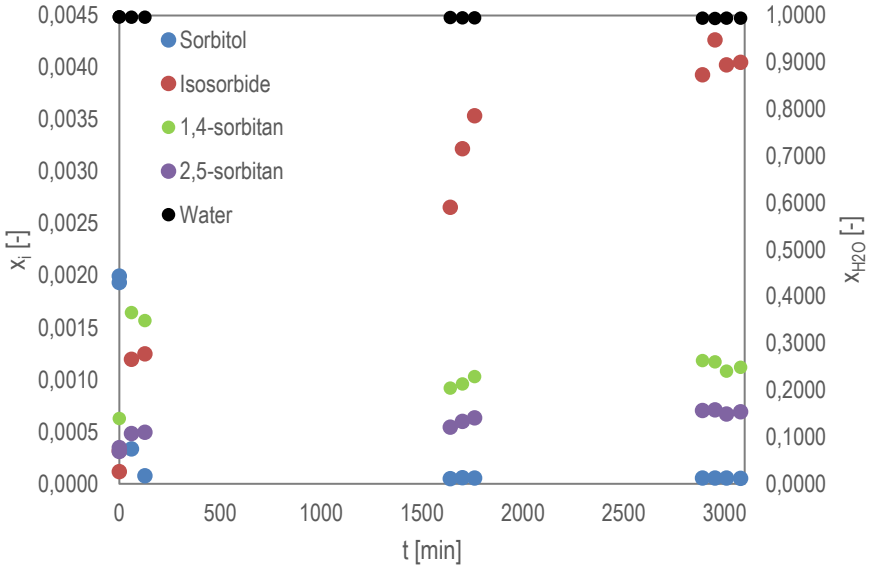

Figure 11. *SOH, IB, 1,4-ST, 2,5-ST, and H_2O mole fraction vs. reaction time (T=170 °C).*

As shown at Figure 11, the equilibrium seems to be reached, despite the oscillations observed at the isosorbide measured data probably originated due to an over pressure at the HPLC column. The evolution of the experiment shows the increasing tendency of the presence isosorbide at the reaction medium as well as the consumption of sorbitol. For the anhydrosorbitols 1,4-sorbitan and 2,5-sorbitan the tendency is quite different., 2,5-sorbitan is formed and not consumed whereas 1,4-sorbitan is formed in a bigger amount but is also consumed in favour of isosorbide formation as also exhibited at Figure 6. It is also observed that the mole fraction of water is nearly constant along the whole experiment, this is explained because the reaction solution is highly diluted in water as also seen at Table 5.

5.2. EXPERIMENTAL EQUILIBRIUM CONSTANT DETERMINATION

The thermodynamic equilibrium constants for the studied reactions (shown at Figure 6) are determined at the previously listed experimental batch runs. The values for those equilibrium constants, being R1 the sorbitol to 1,4-sorbitan dehydration, R2 the 1,4-sorbitan dehydration to isosorbide and R3 the sorbitol to 2,5-sorbitan dehydration reaction. K_1, K_2 and K_3 are the corresponding equilibrium constants for each reaction, obtained with Equations 1 and 2, and listed in Table 7, being $K_{x,1}$, $K_{x,2}$ and $K_{x,3}$ the mole fraction equilibrium constant (Equation 3) and $K_{y,1}$, $K_{y,2}$ and $K_{y,3}$ the non-ideal equilibrium constant correction found with the activity coefficients Modified UNIFAC-Dortmund estimation (Equations 6 to 21).

5.2.1. Activity coefficients Modified UNIFAC-Dortmund estimation

Table 6 shows those activity coefficients for each species and temperature. Calculations are detailed at Appendix 2.

Table 6. *UNIFAC-Dortmund modified method activity coefficients.*

T [K]	γ_{SOH} [-]	γ_{IB} [-]	$\gamma_{1,4\text{-}ST}$ [-]	$\gamma_{2,5\text{-}ST}$ [-]	γ_{H2O} [-]
403,16	3,896	7,568	6,911	3,946	1,001
413,16	3,914	7,800	7,103	3,982	1,001
423,16	4,191	7,628	7,165	4,362	1,000
433,16	4,100	8,076	7,444	4,300	1,000
443,16	4,134	7,882	7,329	4,418	1,000
453,16	4,335	8,117	7,629	4,652	1,000
463,16	3,864	7,851	7,151	4,178	1,000

5.2.2. Experimental equilibrium constants

Table 7 presents the obtained experimental values for the thermodynamic chemical equilibrium constants [K] for each of the studied dehydration reactions.

On one hand, the chemical equilibrium constants values for R1 are far greater than those for R3, which means that the sorbitol dehydration reaction is clearly pathed towards the formation of 1,4-sorbitan instead of 2,5-sorbitan formation, despite being one reaction more favoured than the other, both reaction paths are product (1,4-ST and 2,5-ST) favoured. On the other hand, the equilibrium constants values for R2, despite being the lowest, which means that the 1,4-sorbitan to isosorbide dehydration is the least favoured reaction among the ones studied, are above the unit, so the reaction is product favoured like R1 and R3, which might be really interesting in an industrial scale process, at the reaction conditions previously stated.

As can be seen in Table 7, the equilibrium constant for R1 clearly decreases as temperature increases, which means that the SOH to 1,4-ST dehydration is exothermic whereas R2 and R3 equilibrium constants values slightly increase as temperature increases, which means that both the SOH to 2,5-ST dehydration and the 1,4-ST dehydration are endothermic reactions, this will be discussed later on at 5.3.

Also shown at Table 7, K_y values, especially for R2 and R3 are really close to the unit, which means that the reaction system could be considered as an ideal system, it is also worth to mention that K_y values for R1 suffer a slightly deviation from the ideality, which justifies the usage of the activity coefficients.

Table 7. *Experimental values of the chemical equilibrium constant for each studied reaction.*

Reaction	**T** [K]	**K_x** [-]	**K_y** [-]	**K** [-]
R1	403,16	23,6 ± 2,2	1,77 ± 0,01	42,3 ± 3,9
	413,16	20,88 ± 0,15	1,816 ± 0,003	37,92 ± 0,27
	423,16	21,8 ± 2,3	1,71 ± 0,03	37,3 ± 3,9
	433,16	19,1 ± 2,2	1,82 ± 0,02	35 ± 4
	443,16	21,1 ± 1,5	1,77 ± 0,02	37,4 ± 2,6
	453,16	17,5 ± 4,7	1,76 ± 0,01	30,8 ±8,3
	463,16	17,78 ± 0,18	1,85 ± 0,07	32,92 ± 0,33
R2	403,16	2,44 ± 0,23	1,096 ± 0,005	2,67 ± 0,25
	413,16	3,06 ± 0,08	1,0987 ± 0,0001	3,36 ± 0,09
	423,16	2,33 ± 0,91	1,065 ± 0,006	2,48 ± 0,97
	433,16	3,9 ± 1,1	1,09 ± 0,02	4,3 ± 1,2
	443,16	3,49 ± 0,33	1,076 ± 0,004	3,76 ± 0,36
	453,16	4,29 ± 0,92	1,064 ± 0,003	4,56 ± 0,98
	463,16	4,35 ± 0,39	1,10 ± 0,01	4,78 ± 0,43
R3	403,16	6,46 ± 0,85	1,013 ± 0,002	6,55 ± 0,86
	413,16	6,83 ± 0,08	1,0180 ± 0,0005	6,95 ± 0,08
	423,16	8,7 ± 1,4	1,041 ± 0,005	9,0 ± 1,5
	433,16	12,0 ± 2,9	1,049 ± 0,008	12,6 ± 3,1
	443,16	13,6 ± 2,1	1,07 ± 0,01	14,6 ± 2,3
	453,16	13,1 ± 1,4	1,073 ± 0,008	14,1 ± 1,5
	463,16	12,8 ± 3,3	1,082 ± 0,03	13,8 ± 3,5

5.2.3. Poynting correction factor

The deviation from ideality due to the difference between the standard pressure and the operating pressure is characterized by the Poynting factor like Equation 22 shows. Table 8 summarizes the different values for the Poynting factor for every temperature assayed.

Table 8. *Poynting of the studied reactions at different working temperatures.*

T [K]	$K_{r,1}$	$K_{r,2}$	$K_{r,3}$
403,16	1,013055 ± 0,000008	1,01285 ± 0,00001	1,01312 ± 0,00007
413,16	1,012692 ± 0,000006	1,012543 ± 0,000001	1,012862 ± 0,000002
423,16	1,01238 ± 0,00003	1,01227 ± 0,00001	1,0124 ± 0,0001
433,16	1,012038 ± 0,000003	1,01199 ± 0,00003	1,0122 ± 0,0002
443,16	1,01177 ± 0,00001	1,011729 ± 0,000001	1,01192 ± 0,00006
453,16	1,01149 ± 0,00001	1,011468 ± 0,000004	1,011601 ± 0,00004
463,16	1,01126 ± 0,00005	1,01121 ± 0,00001	1,0115 ± 0,0002

As shown above, the Poynting corrector factor is considerably close to the unit for all the studied reactions, which means that working at high pressure conditions (30 bar) does not affect the thermodynamic equilibrium constants obtained and displayed at Table 7. It is also observed that the calculated Poynting factor oscillates between similar values for all three reactions, this might be seen because the system is extremely diluted in water, thus, water molar volume affects much more than the molar volumes of the rest of the species involved.

5.3. THERMODYNAMIC PROPERTIES

Once the equilibrium constants are known, a representation like Figure 12 is obtained, where van't Hoff linearized equation is presented (Equation 26), in which the natural logarithm of those equilibrium constants are set against the inverse of the temperature (ln(Ki) vs. 1/T [K^{-1}])with its corresponding error.

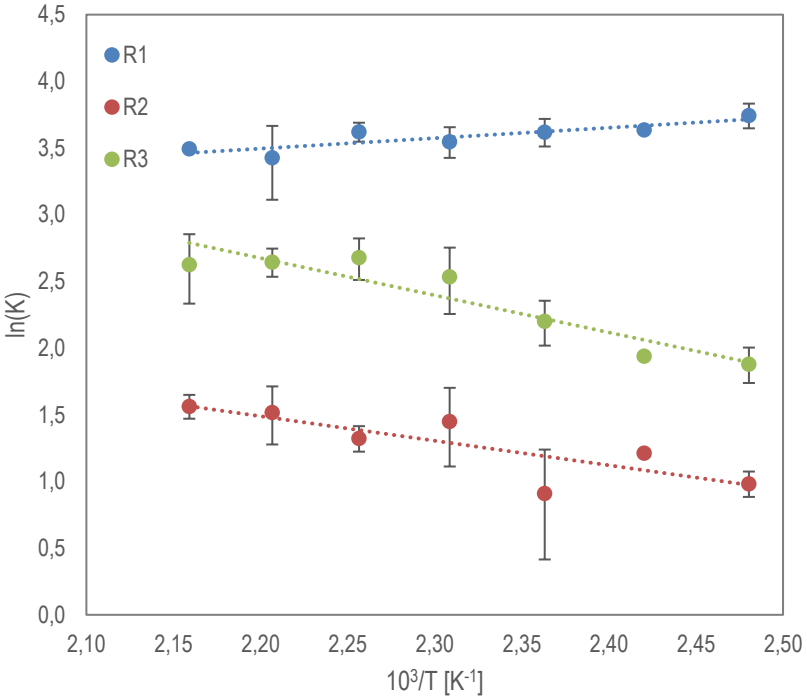

Figure 12. *Van't Hoff plots for the reaction system studied. Dashed lines are linear fits of the experimental data. Error bars correspond to Standard deviation for replicated experiments.*

Following van't Hoff plots the linear regressions of the dehydration reactions, represented at Figure 12, are shown below:

$$\ln(K_1) = (782 \pm 200) \cdot \frac{1}{T} - (1{,}77 \pm 0{,}46) \tag{27}$$

$$\ln(K_2) = (-1838 \pm 561) \cdot \frac{1}{T} - (5{,}5 \pm 1{,}3) \tag{28}$$

$$\ln(K_3) = (-2787 \pm 484) \cdot \frac{1}{T} - (8{,}8 \pm 1{,}1) \tag{29}$$

In order to assure the linearity of the results displayed above, an F-test is realized, Table 9 shows the F value for each one of the regressions as well as the critical F value.

Table 9. *"F" and critical "F" value for each studied reaction van't Hoff linear regression*

Reaction regression	F [-]	Critical "F" value [-]
R1	15,30	0,01
R2	10,74	0,02
R3	33,147	0,002

As presented at Table 9, the critical "F" value for all three linear regressions is lower than 0,05, which means that the linear model has a statistical significance, so exists a significant variability of the dependent variable ($\ln(K_i)$) due to the variability of the dependent variable (1/T).

Once the linearity of the model is assured, the thermodynamical properties can be calculated by the usage of Equation 26. Table 10 shows those calculated properties for the non-ideal reaction system consideration as well as some literature data extracted from [22] and Vasiliu et al. [23], and previous theoretical estimated data extracted from the work titled "Determination of thermodynamic properties of D-sorbitol dehydration to produce D-isosorbide" made by Pau Sales Piñol [24].

Wang et al. [22] studied the thermodynamic calculations and reaction kinetics of the sorbitol dehydration to isosorbide catalysed by N_bOPO_4 were studied in this work. For this authors the thermodynamic analysis, obtained through the concentration equilibrium constant K_c, shows that the two-step dehydration of sorbitol is an endothermic process, in which the first one is an irreversible reaction while the second is a reversible one.

Vasiliu et al. [23] use the G3MP2 computational chemistry method, a high-level approach, was employed to predict the thermodynamic properties of various compounds relevant to the conversion of biomass-derived oxygenated feedstocks into fuels or chemical feedstocks. The initial compounds considered in the study were glucose, 5-hydroxymethyl furfural, sorbitol, levulinic acid, succinic acid, γ-valerolactone, and glycerol. To determine the heats of formation in the liquid phase, the boiling point calculations were combined with the Pictet and Trouton rule, using modified values for ΔS_{vap}.

"Determination of thermodynamic properties of D-sorbitol dehydration to produce D-isosorbide" by Pau Sales Piñol [24] studies the thermodynamics of the double dehydration reaction of

sorbitol to isosorbide. A series of group contribution methods (like Domalski and Hearing, Joback, Vetere, or Růžička and Zábranský) have been considered in order to estimate the thermodynamic parameters of the compounds involved in reaction network. In this work is seen that sorbitol dehydration to both 1,4-sorbitn and 2,5-sorbitan are exothermic whereas the 1,4-sorbitan-to-isosorbide dehydration is endothermic.

Table 10. *Enthalpy and Entropy changes of the reactions in study.*

Reaction	This work[a]		Wang et al.[b] [22]		Vasiliu et al.[c] [23]		Sales Piñol, P. [24]	
	$\Delta_r H°$ [kJ/mol]	$\Delta_r S°$ [J/(mol·K)]	$\Delta_r H°$ [kJ/mol]	$\Delta_r S°$ [J/(mol·K)]	$\Delta_r H°$[d] [kJ/mol]	$\Delta_r S°$ [J/(mol·K)]	$\Delta_r H°$ [kJ/mol]	$\Delta_r S°$ [J/(mol·K)]
R1	-(7 ± 2)	15 ± 4	27,50	---	-23,43	---	-9,14	65,80
R2	15 ± 5	46 ± 11	46,99	---	-29,71[e]	---	57,32	57,99
R3	23 ± 4	73 ± 9	---	---	-37,24	---	-20,56	49,49

[a] Temperature range 403,16-463,16 K. [b] Average properties values for a temperature range between 473,15-533,15 K. [c] Temperature of 298 K. [d] Values in kcal/mol at the original reference, at this table are shown in kJ/mol. [e] This enthalpy value is found as the value for the complete sorbitol-to-isosorbide double dehydration minus the enthalpy value for the first sorbitol dehydration (R1) to 1,4-sorbitan.

Regarding Table 10, the enthalpy change obtained in this experimental workout compared to the values found at the literature [22-23], are approximately on the same magnitude order, however some clear differences can be found. On one hand, in comparison with those values found experimentally by Wang et al., the second dehydration (R2) is endothermic for both studies, despite being both endothermic, the enthalpy change found values are considerably different. For the first dehydration (R1) the deviation in the found values continues and for Wang et al. this first dehydration is also endothermic whereas for this study is found that this reaction has an exothermic behaviour. On the other hand, comparing to those values found by Vasiliu et al. by computational simulation shows that all three studied reactions should behave exothermically whereas what is found experimentally is that only R1 behaves like that. As well as Wang et al. values, these ones are also on the same magnitude order approximately.

To compare this study results with those found by theoretical estimation [24], it is necessary to assume that the heat capacities of the compounds involved remain constant ($\Delta\hat{C}_p \approx 0$) and that the enthalpy variation is constant and not a function of temperature. Estimated values for enthalpy show really interesting approximations for both R1 and R3, not so good for R2, despite that, both R1 and R2 follow the same behaviour for both the estimation model and the experimental work, being exothermic and endothermic, respectively. However, for R3 experimentally is found that the reaction should be endothermic whereas it is found to be exothermic on the estimation study. Moreover, entropies can also be compared between this method and experimental values. Again, both studies' values belong to the same magnitude order, however, especially for R1 and R3, there is a considerable deviation, for R2 this values deviation is not found to be that strong.

Besides the comparison with the literature, a comparison between the considered "ideal" system and the "non-ideal" one is made at Table 11.

Table 11. *Ideal and non-ideal system $\Delta_r H°$ and $\Delta_r S°$ comparison.*

Reaction	Non-ideal system		Ideal system	
	$\Delta_r H°$ [kJ/mol]	**$\Delta_r S°$** [J/(mol·K)]	**$\Delta_r H°$** [kJ/mol]	**$\Delta_r S°$** [J/(mol·K)]
R1	-(7 ± 2)	15 ± 4	-(7 ± 2)	9 ± 4
R2	15 ± 5	46 ± 11	16 ± 4	46 ± 10
R3	23 ± 4	73 ± 9	21 ± 4	69 ± 9

As can be seen at Table 11, the system does not diverge much from the ideality, this might be due to the extreme dilution in water of the reactants present in the system.

Table 12 shows the Gibbs free energy changes for each temperature operated for both “ideal” and “non-ideal” system, obtained by Equation 25.

As for enthalpy and entropy changes, the system does not diverge from ideality when comparing Gibbs free energy change. The found Gibbs free energy changes of the studied reactions is less than 0 for all three, indicating that the both sorbitol dehydration reactions can proceed spontaneously as well as the 1,4-sorbitan dehydration, which means that the reaction, once started, does not need any energy supply. This connects with $\Delta_r S°$ values presented at Table 11. All those $\Delta_r S°$ values are positive ($\Delta_r S° > 0$), which means that the process tends to increase the system disorder, and this processes that increase the disorder are generally favoured, spontaneous ($\Delta_r G° < 0$).

Table 12. *Ideal and non-ideal system $\Delta_r H°$ and $\Delta_r S°$ comparison.*

Reaction	T [K]	Non-ideal system	Ideal system
		$\Delta_r G°$ [kJ/mol]	**$\Delta_r G°$** [kJ/mol]
R1	403,16	-12,5 ± 1,7	-10,5 ± 1,8
	413,16	-12,6 ± 1,7	-10,6 ± 1,8
	423,16	-12,7 ± 1,7	-10,7 ± 1,8
	433,16	-12,9 ± 1,7	-10,8 ± 1,8
	443,16	-13,0 ± 1,7	-10,9 ± 1,8
	453,16	-13,2 ± 1,7	-11,0 ± 1,8
	463,16	-13,3 ± 1,7	-11,0 ± 1,8
R2	403,16	-3,3 ± 4,7	-3,0 ± 4,4
	413,16	-3,7 ± 4,7	-3,4 ± 4,4
	423,16	-4,2 ± 4,7	-3,9 ± 4,4
	433,16	-4,6 ± 4,7	-4,4 ± 4,4
	443,16	-5,1 ± 4,7	-4,8 ± 4,4
	453,16	-5,6 ± 4,7	-5,3 ± 4,4
	463,16	-6,0 ± 4,7	-5,7 ± 4,4
R3	403,16	-6,3 ± 4,0	-6,3 ± 3,9
	413,16	-7,1 ± 4,0	-7,0 ± 3,9
	423,16	-7,8 ± 4,0	-7,7 ± 3,9
	433,16	-8,5 ± 4,0	-8,4 ± 3,9
	443,16	-9,3 ± 4,0	-9,1 ± 3,9
	453,16	-10,0 ± 4,0	-9,7 ± 3,9
	463,16	-10,7 ± 4,0	-10,4 ± 3,9

6. CONCLUSIONS AND FUTURE WORK

The study of the twofold acid-catalysed sorbitol-to-isosorbide reaction system has provided experimental data to determine the equilibrium and the thermodynamic properties of the two dehydration reactions as well as of an important side reaction taken place in the studied system.

Regarding to the equilibrium constant determination, is clear that all three studied reactions, SOH-to-1,4-ST, SOH-to-2,5-ST and 1,4-ST-to-IB, are pathed towards the product formation as can be observed from the mole fraction equilibrium constant values, which are above the unit.

As the equilibrium constant values for sorbitol-to-1,4-sorbitan dehydration are higher than the ones for the 2,5-sorbitan obtention, it is proven that the reaction system evolves to the 1,4-sorbitan formation, which enables the isosorbide formation. In connection with the equilibrium, is remarkable to mention the non-ideality of the mixture. Activity coefficients found are considerably higher than the unit for all the present compounds with the exception of water.

Considering the experimental thermodynamical properties is possible to state that the first sorbitol dehydration (SOH-to-1,4-ST) is exothermic ($\Delta_r H° < 0$) whereas the other two studied reactions are endothermic ($\Delta_r H° > 0$). All three reactions are spontaneous ($\Delta_r G° < 0$) and take place increasing the disorder of the system ($\Delta_r S° > 0$). These enthalpy and entropy changes were estimated to be -(7 ± 2) kJ/mol and (15 ± 4) J/(mol·K) for SOH-to-1,4-ST, (23 ± 4) kJ/mol and (73 ± 9) J/(mol·K) for SOH-to-2,5-ST and (15 ± 5) kJ/mol and (46 ± 11) J/(mol·K) for 1,4-ST-to-IB, respectively.

The obtained thermodynamic results highly disagree with those found in the literature. Notably, literature data (from experimental, computational, or theoretical estimation studies) are contradictory since some conclude that the system is exothermic whereas others conclude that it is endothermic. A possible explanation for these differences could be that the experimental values compared are obtained at different reaction conditions (temperature, pressure, or catalyst), that estimations methods are not quite accurate due to the complexity of the studied molecules, or the consideration of no temperature dependency for the experimental

thermodynamic properties. However, for both the literature and the present study the entropy values are quite similar.

Further work should be focused on studying this system at lower and higher temperatures and with other acid solid catalysts proposed at the literature like other ion-exchange resins or zeolites so as to compare in a more accurate manner the experimental results with the literature and elucidate whether this thermodynamical properties are or not temperature dependant, as well as studying the isohexides formation reactions to expand the knowledge about these systems which may have a great impact on the future industrial and environmentally wise.

REFERENCES AND NOTES

[1] Liguori, F., Moreno-Marrodan, C., & Barbaro, P. (2020). Biomass-derived chemical substitutes for bisphenol A: recent advancements in catalytic synthesis. Journal of Chemical Engineering, 45(2), 123-135.

[2] Narancic, T., Cerrone, F., Beagan, N., & E., K. (2020). Recent Advances in Bioplastics: Application and Biodegradation. Polymers, 12(4), 920. <https://doi.org/10.3390/polym12040920>.

[3] Nanda, S., Patra, B. R., Patel, R., Bakos, J., & Dalai, A. K. (2022). Innovations in applications and prospects of bioplastics and biopolymers: A review. Environmental Chemistry Letters, 20(1), 379-395. <https://doi.org/10.1007/s10311-021-01334-4>.

[4] Zhu, Y., Durand, M., Molinier, V., & Aubry, J.-M. (2008). Isosorbide as a novel polar head derived from renewable resources. Application to the design of short-chain amphiphiles with hydrotropic properties. Journal of Chemical Engineering, 45(3), 234-246. <https://doi.org/10.1039/b717203f>.

[5] García, B., Moreno, J., Morales, G., Melero, J. A., & Iglesias, J. (2020). Production of Sorbitol via Catalytic Transfer Hydrogenation of Glucose. *Applied Sciences*, *10*(5), 1843. <https://doi.org/10.3390/app10051843>.

[6] Soto López, R. (2017). Simultaneous etherification of C4 and C5 iso-olefins with ethanol over acidic ion-exchange resins for greener fuels. Universitat de Barcelona, 24-50.

[7] Castro Santacreu, L. (2022). A contribution to the study of the fructose to isosorbide conversion reaction. Universitat de Barcelona, 7-10.

[8] Benton, M. G., & Dooley, K. M. (Year, Month Day). Vapor-liquid Equilibrium. Retrieved from <https://www.jove.com/es/v/10425/vapor-liquid-equilibrium?language=Arabic#:~:text=An%20activity%20coefficient%20is%20defined,chemical%20potentials%20at%20standard%20states> Accessed on May 23, 2023.

[9] Murphy, B. L. (2015). Chemical Partitioning and Transport in the Environment. In Introduction to Environmental Forensics (Third Edition).

[10] C. Dussenne, T. Delaunay, V. Wiatz, H. Wyart, I. Suisse, and M. Sauthier, “Synthesis of isosorbide: An overview of challenging reactions,” Green Chemistry, vol. 19, no. 22, pp. 5332–5344, 2017, <https://doi.org/10.1039/c7gc01912b>.

[11] M. Yabushita, H. Kobayashi, A. Shrotri, K. Hara, S. Ito, and A. Fukuoka, “Sulfuric acidcatalyzed dehydration of sorbitol: Mechanistic study on preferential formation of 1,4-sorbitan,” Bulletin of the Chemical Society of Japan, vol. 88, no. 7, pp. 996–1002, 2015, <https://doi.org/10.1246/bcsj.20150080>.

[12] Fredenslund, A., Jones, R. L., & Prausnitz, J. M. (1975). Group-Contribution Estimation of Activity Coefficients in Nonideal Liquid Mixtures.
[13] Weidlich, U., & Gmehling, J. (1987). A Modified UNIFAC Model: 1. Prediction of VLE, hE, and ym. Lehrstuhl fur Technische Chemie B, Universitat Dortmund, 0-4600 Dortmund 50, FRG.
[14] Gmehling, J., Li, J., & Schiller, M. (1993). A Modified UNIFAC Model. 2. Present Parameter Matrix and Results for Different Thermodynamic Properties. Ind. Eng. Chem. Res., 32(1), 178-193.
[15] Kang, J. W., Abildskov, J., Gani, R., & Cobas, J. (2002). Estimation of Mixture Properties from First- and Second-Order Group Contributions with the UNIFAC Model. Ind. Eng. Chem. Res., 41(13), 3260-3273.
[16] Skjærseth, J. B.; Andresen, S.; Bang, G.; Heggelund, G. M. The Paris Agreement and Key Actors' Domestic Climate Policy Mixes: Comparative Patterns. Int. Environ. Agreements Polit. Law Econ. 2021, 21, 59−73.
[17] Poiling, B.E.; Prausnitz, J.M.; O'Connel, J.P. "The Properties of GASES AND LIQUIDS". McGraw-Hill, 1959, 5th ed. vol 12. ISBN: 0071499997.
[18] Editors of Encyclopaedia Britannica. "Enthalpy". Encyclopaedia Britannica, 2020. <https://www.britannica.com/science/enthalpy> Accessed on June 2, 2023.
[19] Editors of Encyclopaedia Britannica. "Entropy". Encyclopaedia Britannica, 2020. <https://www.britannica.com/science/entropy-physics> Accessed on June 2, 2023.
[20] https://www.sciencedirect.com/topics/computer-science/thermodynamic-entropy.
[21] Editors of Encyclopaedia Britannica. "Free Energy". Encyclopaedia Britannica, 2020. <https://www.britannica.com/science/free-energy> Accessed on June 2, 2023.
[22] Wang, L., Liu, X., Wang, Y., Sun, W., & Zhao, L. (2022). Thermodynamics and Reaction Kinetics of the Sorbitol Dehydration to Isosorbide Using NbOPO4 as the Catalyst. Industrial & Engineering Chemistry Research, 61(23), 7833-7841.
<https://doi.org/10.1021/acs.iecr.2c00925>
[23] Vasiliu, M., Guynn, K., & Dixon, D. A. (Year). Prediction of the Thermodynamic Properties of Key Products and Intermediates from Biomass. Journal of Biomass Conversion and Biorefinery, 5(2), 103-118. <https://pubs-acs-org.sire.ub.edu/doi/pdf/10.1021/jp204243m>.
[24] Sales Piñol, P. (2022, June). Determination of thermodynamic properties of D-sorbitol dehydration to produce D-isosorbide. Universitat de Barcelona, 27-31.
[25] H. Wyart and M. Ibert, US0092782A1, 2019.
[26] R. Otomo, T. Yokoi, and T. Tatsumi, Appl. Catal., A, 2015, 505, 28–35.
[27] H. Kobayashi, H. Yokoyama, B. Feng, and A. Fukuoka, Green Chem., 2015, 17, 2732–2735.
[28] R. S. Thombal and V. H. Jadhav, Tetrahedron Lett., 2016, 57, 4398–4400.
[29] J. M. Fraile and C. J. Saavedra, ChemistrySelect, 2017, 2, 1013–1018.
[30] J. Shi, Y. Shan, Y. Tian, Y. Wan, Y. Zheng and Y. Feng, RSC Adv., 2016, 6, 13514–13521.
[31] A. Cubo, J. Iglesias, G. Morales, J. A. Melero, J. Moreno and R. Sánchez-Vázquez, Appl. Catal., A, 2017, 531, 151–160.

[32] A. A. Dabbawala, J. J. Park, A. H. Valekar, D. K. Mishra and J. S. Hwang, Catal. Commun., 2015, 69, 207–211.
[33] O. A. Rusu, W. F. Hoelderich, H. Wyart and M. Ibert, Appl. Catal., B, 2015, 176–177, 139–149.
[34] D. Cao, B. Yu, S. Zhang, L. Cui, J. Zhang and W. Cai, Appl. Catal., A, 2016, 528, 59–66.
[35] A. A. Dabbawala, S. M. Alhassan, D. K. Mishra, J. Jegala and J. S. Hwang, Mol. Catal., 2018, 454, 77–86.
[36] J. Deng, B. H. Xu, Y. F. Wang, X. E. Mo, R. Zhang, Y. Li and S. J. Zhang, Catal. Sci. Technol., 2017, 7, 2065–2073.
[37] C. Dussenne, H. Wyart, V. Wiatz, I. Suisse and M. Sauthier, Mol. Catal., 2019, 463, 61–66.
[38] P. Che, F. Lu, X. Si, H. Ma, X. Niea and J. Xu, Green Chem., 2018, 20, 634–640.

ACRONYMS

SOH	Sorbitol
IB	Isosorbide
1,4-ST	1,4-sorbitan
2,5-ST	2,5-sorbitan
IER	Ion-exchange resin
PS-DVB	Polystyrene-divinylbenzene
A-45	Amberlyst-45
CT-482	Purolite CT-482
Γ	Mass-action ratio
a_j	Activity
γ_j	Activity coefficient
x_j	Mole fraction
υ_j	Stoichiometric coefficient
K	Thermodynamic equilibrium constant
K_x	Thermodynamic equilibrium constant referred to the mole fraction
K_γ	Thermodynamic equilibrium constant referred to the activity coefficients
K_Γ	Poynting correction factor
T	Operation temperature [K]
P	Operation pressure [bar] or [atm]
R	Ideal gas constant [(atm·L)/(K·mol)]
V_j	Liquid molar volume [L/mol]
ΔE	Internal energy change [kJ/mol]

$\Delta_r G_i°$	Gibbs free energy change of reaction [kJ/mol]
$\Delta_r H_i°$	Enthalpy change of reaction [kJ/mol]
$\Delta_r S_i°$	Entropy change of reaction [J/mol·K]

APPENDICES

APPENDIX 1: HIGH-PERFORMANCE LIQUID CHROMATOGRAPH

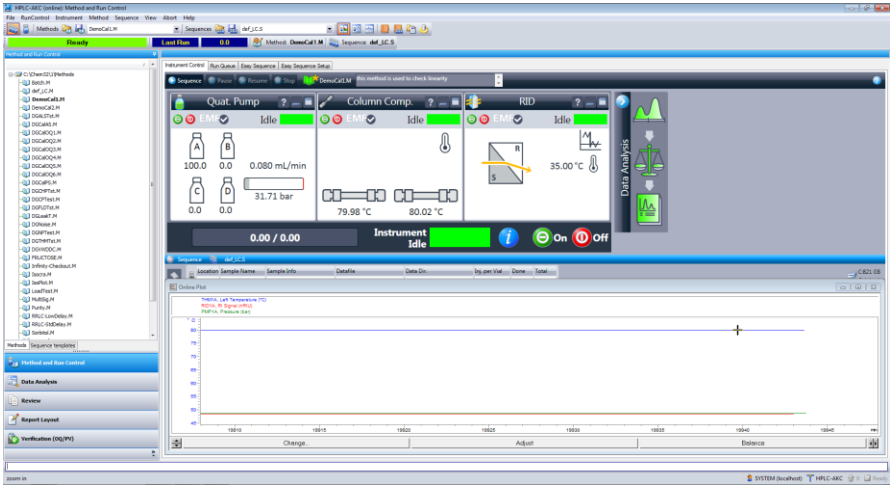

***Figure 13**. HPLC analysis program.*

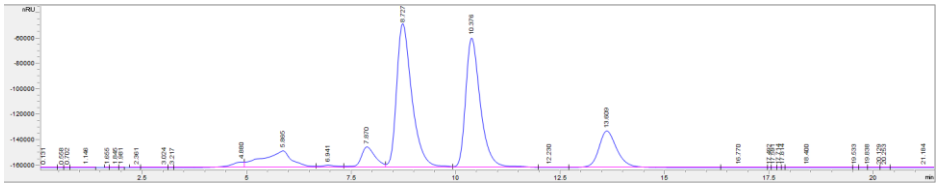

***Figure 14.** Analysis result.*

APPENDIX 2: MODIFIED UNIFAC-DORTMUND ESTIMATION METHOD

In order to find the activity coefficients exposed at Table 6 and consequently K_v on view at Table 7, the Modified UNIFAC-Dortmund estimation method as follows, using Equations from 6 to 21.

Regarding the estimation of those activity coefficients shown, each of the reactants has been deconstructed into the molecular groups considered at the UNIFAC-Dortmund method as follows:

- Sorbitol is deconstructed in 4 secondary OH groups linked to 4 CH groups and 2 primary OH groups linked to 2 CH_2 groups.
- Isosorbide is deconstructed in 4 CH groups, 2 linked to 2 secondary OH groups and the other 2 linked to 2 CH_2O cycled ether group.
- 1,4-sorbitan is deconstructed in 1 CH_2 group linked to a primary OH group, 3 secondary OH groups linked to 3 CH groups and one extra CH group linked to a CH_2O cycled ether group.
- 2,5-sorbitan is deconstructed in 2 CH_2 group linked to 2 primary OH groups, and 4 CH groups, 2 linked to 2 secondary OH groups, and the other 2 linked to the previous 2 CH_2 groups and to a CH_2O cycled ether group.
- Water remains as an H_2O group.

Table 13 shows these groups as well as its corresponding volume (R_k) and surface area (Q_k) values for the combinatorial part calculations.

Table 13. *Tabulated group volume and surface area parameters for the combinatorial part.*

Compound	Contribution Group	$\upsilon_{k,i}$ [-]	R_k [-]	Q_k [-]
SOH	CH_2	2	0,6744	0,5400
	CH	4	0,4469	0,2280
	$OH_{(p)}$	2	1,0000	1,2000
	$OH_{(s)}$	4	1,0000	1,2000
IB	CH	4	0,4469	0,2280
	$OH_{(s)}$	2	1,0000	1,2000
	CH_2O_{cycl}	2	0,2439	0,2400
1,4-ST	CH_2	1	0,6744	0,5400
	CH	4	0,4469	0,2280
	$OH_{(p)}$	1	1,0000	1,2000
	$OH_{(s)}$	3	1,0000	1,2000
	CH_2O_{cycl}	1	0,2439	0,2400
2,5-ST	CH_2	2	0,6744	0,5400
	CH	4	0,4469	0,2280
	$OH_{(p)}$	2	1,0000	1,2000
	$OH_{(s)}$	2	1,0000	1,2000
	CH_2O_{cycl}	1	0,2439	0,2400
H_2O	H_2O	1	0,9200	1,4000

Table 14, 15 and 16 show these groups temperature-dependent interaction parameters values (a_{mn}/a_{nm}, b_{mn}/b_{nm} and c_{mn}/c_{nm}) for the residual part calculations.

Table 14. *Tabulated group temperature-dependent interaction parameters a_{mn}/a_{nm} for the residual part.*

a_{mn}/a_{nm}	CH_2	CH	OH	CH_2O_{cycl}
CH_2	0	174,1	1857	417,6
CH	-157,2	0	2036	269
OH	498,8	-121	0	---[a]
CH_2O_{cycl}	452,2	-305,5	---[a]	0

[a] Not used values due to no interaction CH_2O_{cycl}/OH interaction takes place at any molecule.

Table 15. *Tabulated group temperature-dependent interaction parameters b_{mn}/b_{nm} for the residual part.*

b_{mn}/b_{nm}	CH_2	CH	OH	CH_2O_{cycl}
CH_2	0	-0,5886	-8,653	0,08726
CH	0,6166	0	-8,729	-1,776
OH	-5,1480	-1,901	0	---[a]
CH_2O_{cycl}	-1,997	2,12	---[a]	0

[a] Not used values due to no interaction CH_2O_{cycl}/OH interaction takes place at any molecule.

Table 16. *Tabulated group temperature-dependent interaction parameters c_{mn}/c_{nm} for the residual part.*

c_{mn}/c_{nm}	CH_2	CH	OH	CH_2O_{cycl}
CH_2	0	0	0,01088	0
CH	0	0	0,008138	0,002645
OH	0,01039	0,006999	0	---[a]
CH_2O_{cycl}	0	-0,003239	---[a]	0

[a] Not used values due to no interaction CH_2O_{cycl}/OH interaction takes place at any molecule.